The North African Journal of Scientific Publishing (NAJSP)
مجلة شمال إفريقيا للنشر العلمي (NAJSP)
E-ISSN: 2959-4820
Volume 4, Issue 2, 2026
Page No: 113-120
Website: https://najsp.com/index.php/home/index
SJIFactor 2024: 5.49 **0.69 :2025 (AIF) معامل التأثير العربي** **ISI 2024: 0.696**

Vibration Analysis and Fault Diagnosis of Automotive Suspension Systems

Moamar Hamed[1*], Mohamed Elrawemi[2], Ali Aburass[3], Fengshou Gu[4]
[1]Department of Mechanical and Industrial Engineering, Faculty of Engineering, Alasmarya Islamic University, Zliten, Libya
[2]Department of Mechanical and Industrial Engineering, Faculty of Engineering, Elmergib University, Al-Khums, Libya
[3]Department of Mechanical Engineering Technologies, Higher Institute of Science and Technology, Zawia, Libya
[4]Centre for Efficiency & Performance Engineering, University of Huddersfield, Queensgate, Huddersfield, HD1 3DH, UK

تحليل الاهتزازات وتشخيص أعطال أنظمة تعليق المركبات

معمر احميد[1*]، محمد الرويمي[2]، على أبوراس[3]، فنغشو قو[4]
[1]قسم الهندسة الميكانيكية والصناعية، كلية الهندسة، الجامعة الأسمرية الإسلامية، زليتن، ليبيا
[2]قسم الهندسة الميكانيكية والصناعية، كلية الهندسة، جامعة المرقب، الخمس، ليبيا
[3]قسم تقنيات الهندسة الميكانيكية، المعهد العالي للعلوم والتقنية، الزاوية، ليبيا
[4]مركز هندسة الكفاءة والأداء، كلية الحاسبات والهندسة، جامعة هدرسفلد، المملكة المتحدة

*Corresponding author: m.ehmid@asmarya.edu.ly

Received: February 14, 2026	Accepted: March 29, 2026	Published: April 11, 2026

Abstract:
This paper presents an online condition monitoring strategy for vehicle suspension systems, focusing on the influence of tire pressure at each wheel. The Stochastic Subspace Identification (SSI) method is employed to extract key modal parameters of a full vehicle model, including natural frequencies, damping ratios, and mode shapes. A seven-degree-of-freedom (7-DOF) vehicle model is developed in MATLAB, where vertical acceleration signals measured at the four corners of the vehicle body serve as inputs to the SSI algorithm. Common suspension faults are simulated, particularly tyre under-inflation, by reducing nominal tire pressure by 10%, 20%, 30%, and 40% at individual wheels. Fault detection is achieved by monitoring variations in modal energy, especially those related to bounce and pitch motions. The results indicate that, tyre pressure changes significantly influence the distribution of modal energy within the system. Experimental vibration data under varying pressure conditions further validate the effectiveness and accuracy of the proposed method for early fault detection and suspension condition monitoring.

Keywords: Stochastic Subspace Identification (SSI); Vehicle Suspension Condition Monitoring; Tire Pressure Fault Detection; 7-DOF Vehicle Dynamics Model; Modal Energy Analysis.

الملخص:
تقدم هذه الورقة استراتيجية للمراقبة عن بُعد لحالة أنظمة تعليق المركبات، مع التركيز على تأثير ضغط الإطارات في كل عجلة. تم استخدام طريقة تحديد الفضاء الجزئي العشوائي (SSI) لاستخلاص المعاملات النمطية لنموذج مركبة كامل، والتي تشمل الترددات الطبيعية، ونسب التخميد، وأشكال الاهتزاز. تم تطوير نموذج مركبة بسبع درجات حرية (7-DOF) باستخدام برنامج MATLAB، حيث استُخدمت إشارات التسارع العمودي المقاسة عند الزوايا الأربع لهيكل المركبة كمدخلات لخوارزمية SSI، كما تم محاكاة الأعطال الشائعة في نظام التعليق، وبشكل خاص حالات انخفاض ضغط الإطارات، من خلال تقليل الضغط الاسمي بنسبة 10% و20% و30% و40% في كل عجلة. تم الكشف عن الأعطال من خلال تتبع التغيرات في الطاقة النمطية، خاصة المرتبطة بحركتي الارتداد (bounce) والتأرجح الطولي .(pitch) وأظهرت النتائج أن تغير ضغط الإطارات يؤثر بشكل كبير على توزيع الطاقة النمطية داخل النظام. كما أكدت بيانات الاهتزاز التجريبية تحت ظروف ضغط مختلفة، فعالية ودقة النهج المقترح في الكشف المبكر عن الأعطال ومراقبة حالة نظام التعليق.
الكلمات المفتاحية: طريقة تحديد الفضاء الجزئي العشوائي (SSI)؛ مراقبة حالة نظام التعليق؛ كشف أعطال ضغط الإطارات؛ نموذج ديناميكي للمركبة بسبع درجات حرية؛ تحليل الطاقة النمطية.

Nomenclature:

- $\mathbf{m_s}$: Vehicle body mass or (sprung mass).
- $\mathbf{m_{uf}}$: Front suspension mass or (unsprang mass).
- $\mathbf{m_{ur}}$: Rear suspension mass or (unsprang mass).
- $\mathbf{k_f}$, $\mathbf{k_r}$: Stiffness of front and rear spring.
- $\mathbf{k_{tf}}$, $\mathbf{kt}$: Stiffness of front and rear vehicle tyres.
- $\mathbf{c_f}, \mathbf{c_r}$: Front and rear damper coefficient.
- $\mathbf{\dot{z}_{u1}}, \mathbf{\dot{z}_{u2}}, \mathbf{\dot{z}_{u3}}, \mathbf{\dot{z}_{u4}}$: Velocity of each wheel.
- $\mathbf{l_1}$, $\mathbf{l_2}$: Distance from front and rear wheel to the vehicle center.
- $\mathbf{w_f}, \mathbf{w_r}$: Front and rear vehicle width.
- $\mathbf{\ddot{z}_s}$: Acceleration of the vehicle body.
- $\mathbf{z_{s1}}$, $\mathbf{z_{s2}}$, $\mathbf{z_{s3}}$, $\mathbf{z_{s4}}$: Displacement of the vehicle body at each wheel.
- $\mathbf{z_{u1}}, \mathbf{z_{u2}}, \mathbf{z_{u3}}, \mathbf{z_{u4}}$: Displacement of each wheel.
- $\mathbf{\dot{z}_{s1}}, \mathbf{\dot{z}_{s2}}, \mathbf{\dot{z}_{s3}}, \mathbf{\dot{z}_{s4}}$: Velocity of the vehicle body at each wheel

Introduction:

Inadequate tyre inflation pressure plays a crucial role in affecting vehicle performance, including stability, ride comfort, and braking efficiency, and can also contribute to higher fuel consumption and faster tyre degradation [1][2]. Furthermore, tyre pressure has a direct influence on energy usage and environmental sustainability. The World Energy Outlook (2006) [3] highlights that road transportation represents a major contributor to global energy demand and carbon dioxide (CO_2) emissions. It is estimated that nearly 20% of a vehicle's fuel consumption is used to overcome tyre rolling resistance, underscoring the importance of tyres in overall efficiency. When tyres are under-inflated, rolling resistance increases, which in turn leads to greater fuel usage. Findings from the International Energy Agency Tyre Workshop (2005) [4] reveal that, in practical driving conditions, tyres are frequently under-inflated by approximately 0.2–0.4 bar in passenger vehicles and about 0.5 bar in heavy-duty trucks. Such deviations can result in an increase in energy consumption and CO_2 emissions of around 1–2% for passenger vehicles and approximately 1% for trucks [5].

The effect of tyre pressure on vehicle dynamics has been widely explored in the literature. For example, Al-Solihat et al. [6] analysed how variations in tyre pressure influence both steady state and transient handling characteristics of an urban bus using a three-dimensional vehicle model. Their findings indicated that tyre pressure significantly alters handling performance under different driving conditions. Similarly, Rievaj et al. [7] investigated the link between tyre pressure and braking performance, suggesting that reduced tyre pressure may lead to shorter stopping distances. In another contribution, Persson and Gustafsson [8] introduced an indirect tyre pressure monitoring approach based on vibration analysis and wheel radius estimation, capable of identifying pressure losses greater than 15% within a short time frame. Additionally, Weispfenning [9] proposed a method based on spectral analysis to estimate tyre stiffness and detect pressure changes, demonstrating that vertical wheel acceleration signals alone can provide reliable pressure monitoring.

Extensive research has also been conducted on modelling and evaluating vehicle suspension systems. Faheem [10] developed mathematical representations of both quarter-car (2-DOF) and half-car (4-DOF) models. Rao [11] presented a semi-active quarter-car model with three degrees of freedom to assess skyhook control techniques. Esslaminasa et al. [12] designed a semi-active twin-tube damper model within a quarter-car framework. Darus [13] utilised a state-space formulation in MATLAB to simulate both quarter car and full-vehicle systems. Metallidis [14] applied statistical system identification

techniques for parameter estimation and fault diagnosis in nonlinear suspension systems, while Kashi [15] employed model-based strategies to achieve reliable fault detection and isolation in automotive control systems.

Additional studies have focused on suspension behaviour in relation to ride comfort and handling performance. Agharkakli et al. [16] developed models for both passive and active suspension systems in a quarter-car configuration. Ikenaga et al. [17] proposed an active suspension control strategy based on a full-vehicle model aimed at improving ride quality and road holding capability. Furthermore, Lu et al. [18] examined the effect of vehicle speed on vibration characteristics, demonstrating that root mean square (RMS) acceleration is highly sensitive to speed at lower ranges but becomes less influenced as speed increases.

Despite the well-established importance of tyre pressure in vehicle dynamics, most previous studies have concentrated on aspects such as ride comfort, safety, and fuel economy. However, limited attention has been given to the impact of tyre pressure variations on modal energy characteristics, particularly in the context of detecting suspension faults.

To bridge this gap, the present study introduces an online condition monitoring framework for vehicle suspension systems using the Stochastic Subspace Identification (SSI) technique. The proposed method evaluates how variations in tyre pressure influence vehicle dynamic behaviour through changes in modal energy. Suspension faults are simulated in MATLAB using a seven-degree-of-freedom (7-DOF) full vehicle model by reducing tyre pressure at individual wheels relative to nominal values. These faults are detected by analysing changes in modal energy, with a particular focus on bounce and pitch modes. The validity of the proposed approach is further confirmed through experimental investigations using real measured data.

Suspension System Model and Dynamics:

The mathematical model adopted in this work is based on Ref. [19], with several enhancements introduced to improve its fidelity and ability to represent real vehicle behaviour. Notably, tyre damping has been included to provide a more accurate description of the interaction between the tyres and the road surface. The equations of motion corresponding to each degree of freedom were formulated separately and then combined to obtain a fully coupled set of governing equations describing the dynamics of the vehicle body, as detailed in Hamed et al. [20]. The full-vehicle model configuration employed in this study is illustrated in Figure 1.

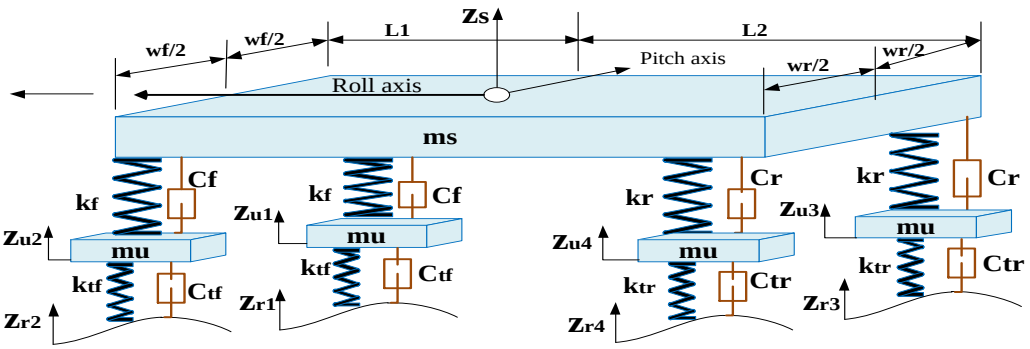

Figure (1): Full Vehicle Models

Equation of motion for bouncing of sprung mass:

$$m_s\ddot{z}_s = k_f(z_{u1} - z_{s1}) + k_f(z_{u2} - z_{s2}) + k_r(z_{u3} - z_{s3}) + k_r(z_{u4} - z_{s4}) + c_f(\dot{z}_{u1} - \dot{z}_{s1}) + c_f(\dot{z}_{u2} - \dot{z}_{s2}) + c_r(\dot{z}_{u3} - \dot{z}_{s3}) + c_r(\dot{z}_{u4} - \dot{z}_{s4}) \quad (1)$$

For pitching moment of inertia of sprung mass:

$$I_p\ddot{\theta} = k_f l_1(z_{u1} - z_{s1}) + k_f l_1(z_{u2} - z_{s2}) - k_r l_2(z_{u3} - z_{s3}) - k_r l_2(z_{u4} - z_{s4}) + c_f l_1(\dot{z}_{u1} - \dot{z}_{s1}) + c_f l_1(\dot{z}_{u2} - \dot{z}_{s2}) - c_r l_2(\dot{z}_{u3} - \dot{z}_{s3}) - c_r l_2(\dot{z}_{u4} - \dot{z}_{s4}) \quad (2)$$

For rolling motion of the sprung mass:

$$I_r\ddot{\varphi} = \frac{k_f w_f}{2}(z_{u1} - z_{s1}) - \frac{k_f w_f}{2}(z_{u2} - z_{s2}) + \frac{k_r w_r}{2}(z_{u3} - z_{s3}) - \frac{k_r w_r}{2}(z_{u4} - z_{s4}) + \frac{c_f w_f}{2}(\dot{z}_{u1} - \dot{z}_{s1}) - \frac{c_f w_f}{2}(\dot{z}_{u2} - \dot{z}_{s2}) + \frac{c_r w_r}{2}(\dot{z}_{u3} - \dot{z}_{s3}) - \frac{c_r w_r}{2}(\dot{z}_{u4} - \dot{z}_{s4}) \quad (3)$$

For each wheel motion in vertical direction:

$$m_{uf}\ddot{z}_{u1} = -k_f(z_{u1} - z_{s1}) - c_f(\dot{z}_{u1} - \dot{z}_{s1}) + k_{tf}(z_{r1} - z_{u1}) + ctf(\dot{z}_{r1} - \dot{z}_{u1}) \quad (4)$$

$$m_{uf}\ddot{z}_{u2} = -k_f(z_{u2} - z_{s2}) - c_f(\dot{z}_{u2} - \dot{z}_{s2}) + k_{tf}(z_{r2} - z_{u2}) + ctf(\dot{z}_{r2} - \dot{z}_{u2}) \quad (5)$$

$$m_{ur}\ddot{z}_{u3} = -k_r(z_{u3} - z_{s3}) - c_r(\dot{z}_{u3} - \dot{z}_{s3}) + k_{tr}(z_{r3} - z_{u3}) + ctr(\dot{z}_{r3} - \dot{z}_{u3}) \quad (6)$$

$$m_{ur}\ddot{z}_{u4} = -k_r(z_{u4} - z_{s4}) - c_r(\dot{z}_{u4} - \dot{z}_{s4}) + k_{tr}(z_{r4} - z_{u4}) + ctr(\dot{z}_{r4} - \dot{z}_{u4}) \quad (7)$$

The vertical displacements at the four corners of the vehicle's sprung mass (1, 2, 3, and 4 shown in Fig. 1), located directly above the corresponding unsprung masses, **can be expressed as follows:**

$$Zs1 = Zs - L1\theta + (wf / 2)\varphi \quad (8)$$

$$Zs2 = Zs - L1\theta - (wf / 2)\varphi \quad (9)$$

$$Zs3 = Zs + L2\theta + (wr / 2)\varphi \quad (10)$$

$$Zs4 = Zs + L2\theta - (wr / 2)\varphi \quad (11)$$

The variables used in the model equations were defined and summarized in the nomenclature section, along with the suspension system parameters. An exception was made for the tyre damping coefficients associated with different inflation pressures, which were adopted from Ref. [19]. In addition, certain variables were adjusted to align with the specifications of the experimental vehicle used in this study.

The system dynamics were represented in state-space form, as described in a previous study conducted by the first author and co-authors [20]. To simulate the state-space model, a program was developed using MATLAB to generate and analyse the system matrices. The vehicle parameters and their corresponding values are presented in Table (1).

Table (1): Vehicle parameters and their corresponding values.

Parameters	Symbol	Value	Unit
Mass of the vehicle	m_s	1480	Kg
Front mass	m_{uf}	40.5	Kg
Rear mass	m_{ur}	40.5	Kg
Stiffness of front suspension	k_f	21500	N/m
Stiffness of rear suspension	k_r	19500	N/m
Coefficient of front shock absorber	c_f	1400	N.s/m
Coefficient of rear shock absorber	c_r	1400	N.s/m
Front tyre stiffness	k_{tf}	190900	N/m
Rear tyre stiffness	k_{tr}	190900	N/m
Pitching moment inertia of the vehicle	I_p	360	Kg m^2
Rolling moment inertia of the vehicle	I_r	2200	Kg m^2
Distance from the CG of the car to front axle	l_1	1.4	m
Distance from the CG to the rear axle	l_2	1.4	m
Half width of the front axle	w_f	0.7	m
Half width of the rear axle	w_r	0.7	m

Subspace-Based System Identification for Suspension System:

Previous studies by Dong et al. [19] and Hamed et al. [20] have provided comprehensive explanations of subspace identification techniques and their mathematical formulations. Dong et al. [19] estimated a vehicle's modal properties and mass moments of inertia by analysing acceleration data from both sprung and unsprung masses using subspace-based methods. Their research compared two strategies: one incorporating both input and output data, and another based solely on output measurements, with particular attention to highly damped modes. The results showed that, at lower vehicle speeds, employing unsprung mass accelerations as inputs leads to more accurate identification than using road–tyre interaction forces. Additionally, the study highlighted that real-time estimation of vehicle parameters is achievable through the analysis of roll and yaw motions.

In a related study, Hamed et al. [20] focused on detecting suspension faults by modelling different levels of damper degradation (25%, 50%, and 80%) within a nonlinear full-vehicle framework. They applied the Stochastic Subspace Identification (SSI) approach to acceleration data of the sprung mass to identify bounce, pitch, and roll modes without relying on tyre force inputs. Their findings demonstrated high accuracy in estimating natural frequencies, while damping ratio estimates showed some variability. Overall, the results support the effectiveness of SSI methods for identifying suspension characteristics and diagnosing faults.

Experimental Investigation:

The test vehicle used in this study is a Vauxhall Zafira, a five-door multi-purpose vehicle (MPV) with a front-wheel-drive (FWD) configuration. It has an overall length of 4317 mm, a width of 1742 mm, and a height of 1634 mm, with a wheelbase of 2694 mm. The curb weight of the vehicle is approximately 1448 kg. To replicate realistic operating conditions during the experimental work, an additional load equivalent to two persons (approximately 150 kg) was added to the total vehicle weight.

The experimental study was then carried out to measure the accelerations at the four corners of the vehicle. Four vibration sensors were installed and connected to a four-channel data acquisition system, as illustrated in Figure (2).

(4) Accelerometers

4- Channels Data Acquisition System

(4) Amplifiers

Laptop Computer

Figure (2): Measurement System Devices

Vibration measurements were performed using four piezoelectric accelerometers (model CA-YD-104T). The sensors have sensitivities of 3.243, 3.77, 3.573, and 3.64 pc/ms^{-2}, respectively. Each sensor operates within a frequency range of 0.5–7000 Hz, ensuring adequate coverage of the vehicle's dynamic response. In addition, the sensors are designed to operate within a temperature range of −20 to 120 °C, making them suitable for the experimental conditions.

Results and Discussion:

Results of Subspace Identification for the 7-DOF Vehicle Model:

In the simulation study, the outputs of the 7-DOF vehicle model (specifically the body motions at the four vehicle corners) were used as input data for the SSI model. The identified modal parameters, including natural frequencies, damping ratios, and mode shapes, were then evaluated by comparing them with the corresponding results of the original 7-DOF system. Based on this comparison, the extracted parameters are suitable for use in online suspension condition monitoring. The natural frequencies f_n and damping ratios ζ_i for the 7-DOF vehicle model were presented in Table 2.

Table (2): Undamped natural frequency f_n and damping ratio ζ_i for the 7-DOF vehicle model.

Mode	1(bounce)	2(pitch)	3(roll)	4(fl-w)	5(fr-w)	6(rl-w)	7(rr-w)
$f_n\ (Hz)$	1.0793	1.294	1.595	10.840	10.840	11.532	11.532
ζ_i	0.212	0.2474	0.3079	0.2314	0.232	0.2438	0.2439

Figure 3 illustrates the frequency response and corresponding mode shapes of the vehicle body for bounce, pitch, and roll motions under baseline conditions (i.e., without any change in tyre inflation pressure). The bounce mode occurs at a natural frequency of approximately 1.043 Hz with a damping ratio of 20.21%, and its mode shape is characterized primarily by vertical translational motion of the vehicle body.

The pitch mode is observed at a natural frequency of approximately 1.285 Hz and a damping ratio of 24.37%. Its mode shape represents rotational motion about the vehicle's lateral axis, where the front and rear sections move vertically in opposite directions. The roll mode is observed at a natural frequency of approximately 1.587 Hz with a damping ratio of 30.32%. Its mode shape reflects rotation about the longitudinal axis, which is orthogonal to the pitch motion. Compared with bounce and pitch, the roll mode exhibits both a higher natural frequency and damping ratio, indicating a stronger contribution of lateral rotational dynamics to the overall vehicle response in the simulation.

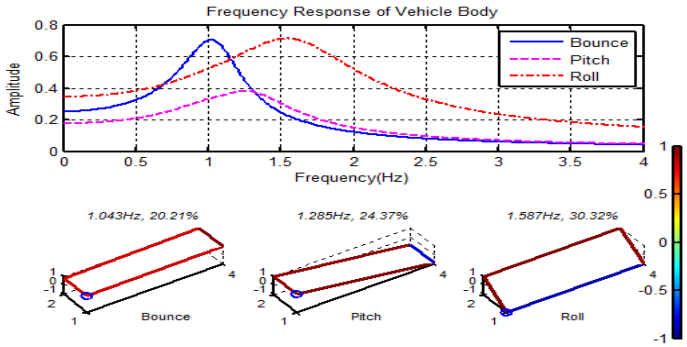

Figure (3): Frequency response and mode shapes of the bounce pitch and roll mode.

Tyre Pressure Change Results:

In the simulation study, suspension faults were introduced by varying tyre inflation pressure under some operating conditions: the nominal pressure (2.2 bar) and cases where the front-left tyre was under-inflated by 10%, 20%, 30% and 40% relative to the standard value. Figure 4 presents the corresponding variations in natural frequency, damping ratio, and mode shapes for the bounce and pitch modes under these conditions.

The results indicate that the natural frequencies of all three modes, bounce, pitch and roll, decrease progressively as the front-left tyre pressure is reduced by 10%, 20%, and 30%. and 40% Similarly, the damping ratios exhibit a decreasing trend with increasing levels of under-inflation. In contrast, the mode shapes show a gradual increase in their response magnitude under the same fault conditions, reflecting a growing alteration in the dynamic behavior of the system as tyre pressure decreases.

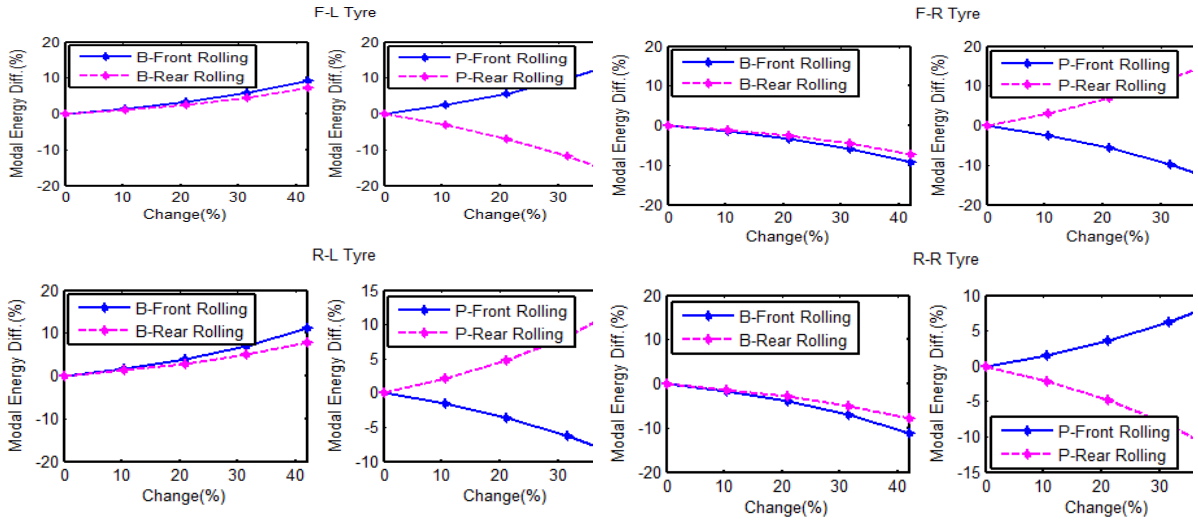

Figure (4): Variation of natural frequency, damping ratio, and mode shapes for bounce and pitch across a range of tyre pressures.

Experimental Results using Stochastic Subspace Identification Methods:

The primary objective of the experiment was to acquire the vibration (acceleration) response of the vehicle body at its four corners, enabling a detailed assessment of the influence of tyre under-inflation on the bounce, pitch, and roll dynamics of the vehicle. The tests were conducted under different conditions: the nominal pressure of 2.2 bar, and cases in which the front-left tyre was under-inflated by 10%, 20%, 30% and 40% relative to the standard value. All measurements were carried out at a constant vehicle speed of approximately 40 km/h.

Figure 5 presents the mode selection based on the frequency-to-order ratio for three conditions: the baseline case (2.2 bar, top plot), 20% under-inflation (middle plot), and 30% under-inflation (bottom plot) of the front-left tyre. The results show a slight reduction in the low-frequency range associated with the vehicle body dynamics (approximately 1–3 Hz) as tyre pressure decreases to 20% and 30% under-inflation, respectively.

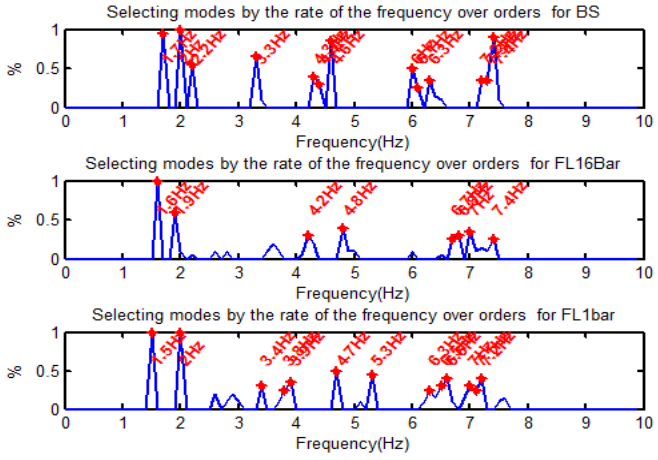

Figure (5): Mode selection based on frequency variation across orders for the baseline case (2.2 bar) and front-left wheel under-inflation cases (1.6 bar and 1.0 bar)..

Figure 6 presents the vehicle body mode shapes together with the corresponding vibration energy distribution. It can be observed that the dominant responses in most test cases are associated with bounce and pitch motions. In contrast, roll motion does not appear as a clearly isolated mode and, in several cases, is coupled with pitch motion, making it difficult to distinguish as an independent dynamic response.

This behavior suggests that inward roll is present when the roll axis is positioned above the vehicle center of gravity (CG), which does not adversely affect vehicle stability. According to the definition provided by the Society of Automotive Engineers (SAE), the roll center is the point at which a lateral force can be applied without inducing body roll. Consequently, if the roll center coincides with the center of gravity, no body roll would occur under lateral loading conditions.

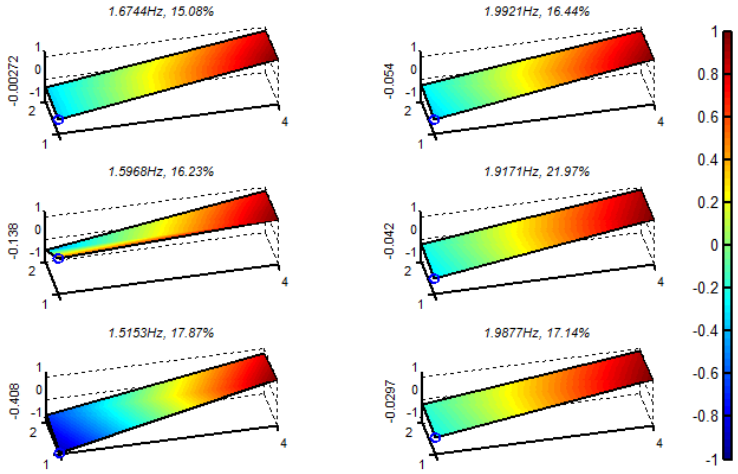

Figure (6): Mode shapes of the vehicle body

Figure 7 shows the variation of modal energy for the front and rear rolling modes of the vehicle body under different tyre pressure conditions. The results indicate that the front rolling mode, with a frequency of 1.67 Hz and a damping ratio of 15.1%, remains essentially unchanged under baseline conditions and for tyre pressure reductions of 0% to 10%. However, when the front left tyre is under-inflated by 20% to 40%, the modal energy of the front rolling mode increases to approximately 0.2%. In this case, the natural frequency decreases slightly to 1.6 Hz, while the damping ratio increases to 16.2%. For further under-inflation in the range of 45% to 65%, the modal energy continues to rise, reaching about 0.4%, accompanied by a further reduction in frequency to 15.2 Hz. In contrast, the modal energy of the rear rolling mode remains unaffected throughout all tests, as no pressure changes were applied to the rear tyres.

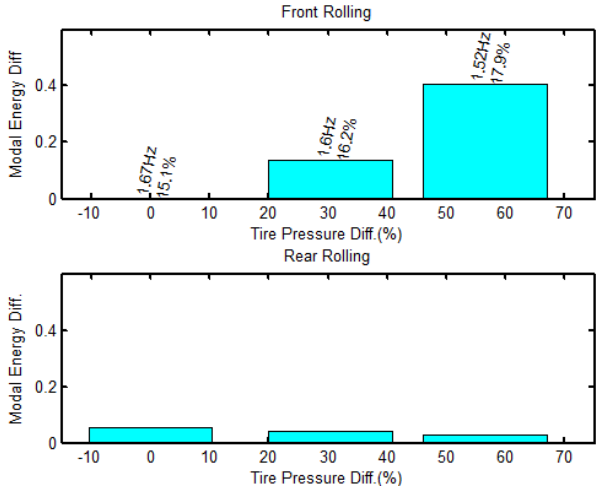

Figure (7): modal energy differences verses tyre pressure changes for front and rear rolling mode

Conclusion:

This study presented the application of Stochastic Subspace Identification (SSI) techniques for estimating vehicle modal parameters, including natural frequencies, damping ratios, and mode shapes, based on experimental output data and MATLAB simulations of a seven-degree-of-freedom (7-DOF)

full vehicle model. The effect of tyre inflation pressure variations on the vehicle's modal behavior was also investigated.

The simulation results indicate that reducing tyre pressure leads to a decrease in the natural frequencies associated with the vehicle body's bounce, pitch, and roll modes. Moreover, under-inflated tyres were found to lower the damping ratios of these vibration modes. Variations in tyre pressure were also observed to affect the corresponding mode shapes. The SSI-based modelling approach showed strong capability in estimating the vehicle's modal properties, providing a reliable basis for the development of online condition monitoring systems for automotive suspension applications. Experimental results obtained from the test vehicle followed similar trends and were in good agreement with the simulation outcomes.

References:

1. Hamed, M., Tesfa, B., Gu, F., & Ball, A. (2014, July). Effects of tyre pressure on vehicle suspension performance. In World Symposium on Mechanics Engineering & Applied Physics (WSMAEP'14).
2. Belayneh, N., Nallamothu, R. B., Nallamothu, A. K., & Nallamothu, S. K. (2021). Effect of Tyre Inflation Pressure on Fuel Consumption and Vehicle Handling Performance. In Advances in Fluid and Thermal Engineering: Select Proceedings of FLAME 2020 (pp. 607-617). Singapore: Springer Singapore.
3. International Energy Agency, "World Energy Outlook 2006," 2006.
4. International Energy Agency, "Fuel Efficient Road Vehicle Non-Engine Components," 2007.
5. Jette Krause,et all ,EU road vehicle energy consumption and CO2 emissions by 2050 – Expert-based scenarios, Energy Policy, Volume 138, 2020,111224,ISSN 0301-4215.
6. M. K. Al-Solihat, S. Rakheja, and A. K. W. Ahmed, "Influence of tyre pressure on an urban bus transient and steady state handling performance," Proc. Inst. Mech. Eng. Part J. Automob. Eng., vol. 224, no. 7, pp. 893–908, 2010.
7. V. Rievaj, "Tire Inflation Pressure Influence on a Vehicle Stopping Distances," Int. J. Traffic Transp. Eng., no. 2 (2), pp. 9–13, 2013.
8. F. Gustafsson, N. Persson, and M. Drevö, "Indirect Tire Pressure Monitoring using Sensor Fusion," presented at the Proceedings of the SAE 2002 World Congress, 2002.
9. T. Weispfenning, "Fault Detection and Diagnosis of Components of the Vehicle Vertical Dynamics," Meccanica, vol. 32, no. 5, pp. 459–472, Oct. 1997.
10. Ahmad Faheem, Fairoz Alam, and V. Thomas, "The suspension dynamic analysis for a quarter car model and half car model," Dec-2006
11. R. Rao, T. Ram, k Rao, and P. Rao, "Analysis of passive and semi active controlled suspension systems for ride comfort in an omnibus passing over a speed bump," Oct-2010
12. N. Eslaminasab, M. Biglarbegian, W. W. Melek, and M. F. Golnaraghi, "A neural network based fuzzy control approach to improve ride comfort and road handling of heavy vehicles using semi-active dampers," Int. J. Heavy Veh. Syst., vol. 14, no. 2, pp. 135–157, Jan. 2007.
13. R. Darus and Y. M. Sam, "Modeling and control active suspension system for a full car model," in 5th International Colloquium on Signal Processing Its Applications, 2009. CSPA 2009, 2009, pp. 13–18.
14. P. Metallidis, G. Verros, S. Natsiavas, and C. Papadimitriou, "Fault Detection and Optimal Sensor Location in Vehicle Suspensions," J. Vib. Control, vol. 9, no. 3–4, pp. 337–359, Mar. 2003.
15. K. Kashi, D. Nissing, D. Kesselgruber, and D. Soffker, "Diagnosis of active dynamic control systems using virtual sensors and observers," in 2006 IEEE International Conference on Mechatronics, 2006, pp. 113–118.
16. A. Agharkakli, G. Sabet, and A. Barouz, "Simulation and Analysis of Passive and Active Suspension System Using Quarter Car Model for Different Road Profile," Int. J. Eng. Trends Technol.-, vol. 3, no. 5, 2012.
17. S. Ikenaga, F. L. Lewis, J. Campos, and L. Davis, "Active suspension control of ground vehicle based on a full-vehicle model," in American Control Conference, 2000. Proceedings of the 2000, 2000, vol. 6, pp. 4019–4024 vol.6.
18. F. Lu, Y. Ishikawa, H. Kitazawa, and T. Satake, "Effect of vehicle speed on shock and vibration levels in truck transport," Packag. Technol. Sci., vol. 23, no. 2, pp. 101–109, 2010.
19. G. Dong, J. Chen, and N. Zhang, "Investigation into on-road vehicle parameter identification based on subspace methods," J. Sound Vib., vol. 333, no. 24, pp. 6760–6779, Dec. 2014.
20. Moamar Hamed, Ali M. Aburass, & Fengshou Gu. (2024). Subspace-Based System Identification and Fault Detection for Suspension System Based on Vibration Analysis. Afro-Asian Journal of Scientific Research (AAJSR), 2(2), 16-32.